ON THE SEMI-ACTIVE CONTROL METHOD FOR TORSIONAL VIBRATIONS IN ELECTRO-MECHANICAL SYSTEMS BY MEANS OF ROTARY ACTUATORS WITH A MAGNETO-RHEOLOGICAL FLUID

Agnieszka Pręgowska, Robert Konowrocki, Tomasz Szolc

Institute of Fundamental Technological Research of the Polish Academy of Sciences, Warsaw, Poland
e-mail: aprego@ippt.gov.pl; rkonow@ippt.gov.pl; tszolc@ippt.gov.pl

The aim of this paper is to present a method of the semi-active control of torsional vibrations in a working machine drive system by means of rotary actuators with a magneto-rheological fluid. The simple open-loop control strategy is proposed for a mechanical system vibrating in steady-state operating conditions. This semi-active control approach is based on the principle of optimum viscous damping and frictional properties realized by the magneto-rheological fluid, where its respective parameters are determined by the applied control electric currents. The analysis is performed theoretically by means of structural electro-mechanical models of the considered drive system as well as experimentally using a laboratory test rig in the form of a rotor-shaft system co-operating with two asynchronous motors generating properly programmed driving and retarding electro-magnetic torques.

Key words: semi-active control, torsional vibrations, magneto-rheological rotary dampers

1. Introduction

Torsional vibrations of drive systems of machines, mechanisms and vehicles are a source of additional oscillatory angular displacements superimposed to nominal rotational motions of a considered object. On the one-hand, this phenomenon results in severe dynamic overloads leading to dangerous shaft and coupling material fatigue, in too fast wear of gear stage teeth as well as in harmful noise generation and unexpected loss of transmitted energy. On the other hand, during regular exploitation conditions, torsional vibrations are hardly detectable and, contrary to lateral and axial vibrations of the drive systems, they are difficult to measure and monitor. The applied so far passive methods of attenuation of torsional vibrations are not sufficiently effective in majority of practical applications. Here, it is to emphasize that torsional vibrations are in general rather difficult to control not only from the viewpoint of proper control torque generation, but also from the point of view of a convenient technique of imposing the control torques on quickly rotating parts of the drive-systems.

Recently observed fast development of active and semi-active control strategies for mechanical systems opens new possibilities for suppressing this detrimental phenomenon. Nevertheless, one can find not so many published results of research in the field of attenuation of torsional vibrations, beyond some attempts performed by active control using piezo-electric actuators, Przybyłowicz (1995). But in such cases, relatively small values of control torques can be generated, and thus the piezo-electric actuators can be usually applied to low-power drive systems. Moreover, even if a relatively big number of piezo-electric actuators are attached to shafts of the entire drive system, as it follows e.g. from Przybyłowicz (1995), only higher eigenmodes can be controlled, whereas control of the most important fundamental eigenmodes is often not sufficiently effective. As it follows e.g. from Spencer *et al.* (1997) and Wang and Meng (2005), an application of dampers with the magneto-rheological fluid (MRF) enables effective suppression of vibrations in several mechanical systems. The MRFs are functional fluids whose effective

viscosity depends on the externally provided magnetic field. This feature makes them perfectly suitable for large brakes and clutches with controllable damping characteristic. Besides the ability to generate large damping torques, an important advantage of the MRF-based devices is low power consumption. External power is needed to supply the electro-magnetic windings only, i.e. to modify the dynamic characteristics of the mechanical system, which is the distinguishing feature of the semi-active control. Moreover, the semi-active damping-based approach eliminates the risk of instability, which is intrinsically related to the active control paradigm and which could potentially occur in the case of electrical failure, unexpected control time delays or in the case of inaccurate modelling. In addition, it should be remarked that, as demonstrated in Mikułowski and Holnicki-Szulc (2007), there exist effective control methodologies based on actuators with the MRF, which are characterized by actual control delays reaching few milliseconds only. Thus, this technique enables us to control effectively vibrations of a frequency exceeding 100 Hz or more. Nevertheless, in the abovementioned and numerous other papers, this technique has been used for semi-active control of vibrations characterized by translatory motions. However, in Szolc *et al.* (2011, 2013), a semi-active torsional vibration control technique based on the actuators in the form of linear dampers with the MRF co-operating with the visco-elastically rotationally suspended planetary gear housing is proposed. Here, be means of on-line programmable viscosity of the MRF, one can effectively suppress transient and steady-state torsional vibrations occurring in a wide class of drive systems. But this approach requires an application of complex and expensive devices, which is particularly troublesome in the case of drive systems in which gear stages are not necessary. According to the above, in Szolc *et al.* (2010) and Pręgowska *et al.* (2012), the advantages of the MRF were used for another, simpler concept of rotary actuators applied for attenuation of torsional vibrations. In papers by Szolc *et al.* (2010) and Pręgowska *et al.* (2012), the actuating technique is based on rotary dampers and realized in an analogous way to the known torsional vibration viscous dampers installed on crankshafts of the reciprocating engine. But here, instead of the silicon oil between the shaft and the inertial ring, which can freely rotate with a velocity close or equal to the system average rotational speed, the MRF of an adjustable viscosity is used. Such actuators generate control torques that are functions of the difference between the rotational speeds of the rings and of the shaft, where the latter consists of the average component corresponding to the rigid body motion and of the fluctuating component caused by the torsional vibrations. Since the average rotational speeds of the rings and of the shaft are similar, only small wearing effects can be expected, and the vibrations can be suppressed without influencing much the rigid body motion of the drive system. In these papers introductory investigations for several concepts of semi-active control strategies were successfully performed.

In the present paper, the semi-active control of torsional vibrations is also going to be carried out by means of the abovementioned rotary dampers with the MRF, where more thorough attention will be focused on experimental verification of theoretical findings as well as on modelling of the MRF.

2. Description of the torsionally vibrating drive system with magneto-rheological dampers

In order to elaborate semi-active control techniques for attenuation of torsional vibration, a proper laboratory drive system equipped with rotary dampers with an MRF has been built. In the considered laboratory drive system the power is transmitted from a servo-asynchronous motor to the driven machine in form of a programmable electric brake by means of two multi-disk elastic couplings with built-in torque-meters, electro-magnetic overload coupling and by shaft segments. Moreover, this system contains two rotary magneto-rheological dampers and

two inertial disks of adjustable mass moments of inertia and axial positions, which enable us to tune-up the drive train to a proper natural frequency. The considered real laboratory drive system together with a photograph of the magneto-rheological damper is presented in Fig. 1. The scheme of this damper has been shown in Fig. 2. Moreover, the described above test-rig is equipped with a proper measurement-control system, the scheme of which presents Fig. 3. This system consists of a voltage amplifier controlled by a real-time computer using the appropriate converting system. Such a measurement control system enables us to monitor and register all results of measurements using the control-communication unit by means of the TCP/IP protocol. Basing on the measurement results of the dynamic torques obtained on-line and transmitted by the shaft segments adjacent to the torque-meters shown in Fig. 1, the properly developed control algorithm is able to determine in real time the current values of damping coefficients of the MRF in both rotary dampers.
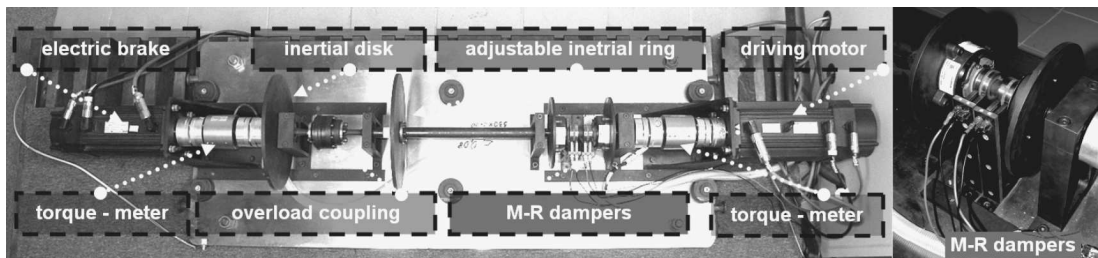

Fig. 1. Laboratory drive system with the magneto-rheological dampers
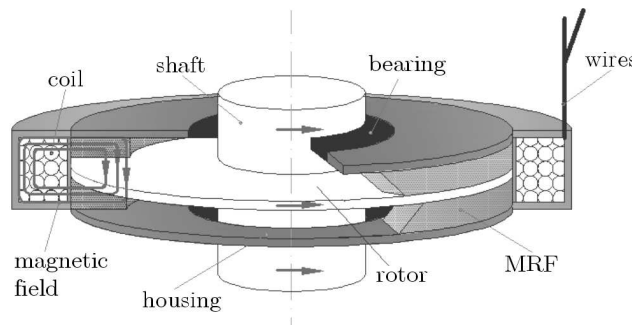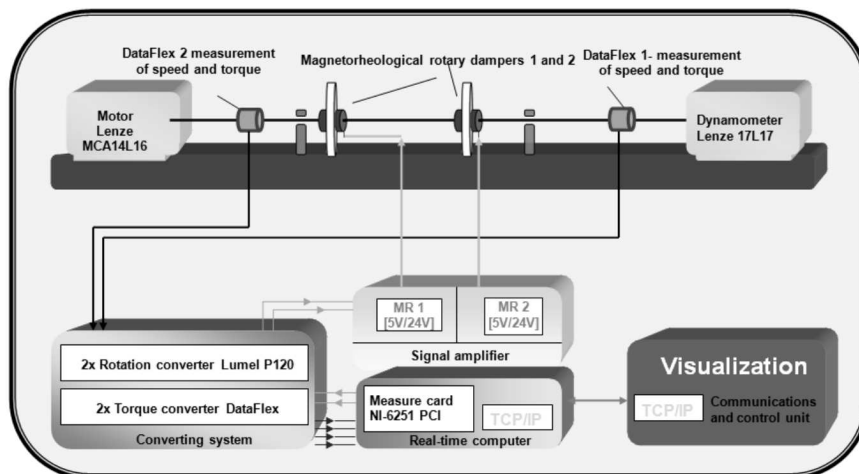

Fig. 2. Rotary damper with the MRF

Fig. 3. Scheme of the test-rig measurement system

For the purpose of numerical simulations of the proposed concept of semi-active control of torsional vibrations, an experimental identification of magneto-rheological damper dynamic properties is very important. Such results will be applied for proper theoretical modelling of this device. Here, the fundamental role is played by the appropriately assumed and identified rheological model of the MRF which in the case of rotary damper is affected by a shearing mode of activity. For this aim, several models of such magneto-rheological rotary devices have been built, Makowski *et al.* (2011) and Gorczyca and Rosół (2011). In all of them, the Bingham model of the MRF is applied. Both in Makowski *et al.* (2011) and in Gorczyca and Rosół (2011), the dynamic properties of the MRF are regarded as a parallel combination of a viscous and frictional damper. In the presented paper, the rotary dampers have been built using the commercial magneto-rheological rotary brakes RD 2087-01 made by LORD Company, as can be seen on the photograph in Fig. 1. The rheological properties of this brake were experimentally identified by Gorczyca and Rosół (2011). By means of those identification results, the following simple mathematical description of the damping torque generated by this device has been proposed

$$M_D\big(i(t)\big) = -M_D^F\big(i(t)\big)\operatorname{sgn}\big(\Delta\Omega(t)\big) - d\big(i(t)\big)\Delta\Omega(t) \tag{2.1}$$

where $M_D^F(i(t))$ and $d(i(t))$ denote, respectively, the control electric current dependent static frictional damping torque component and the viscous damping coefficient of the MRF, $\Delta\Omega(t)$ is the difference between angular velocities of the torsionally vibrating shaft and the rotary brake housing or the rotary damper inertial ring, and $i(t)$ denotes the programmable, time-dependent control electric current in device coils. The identified by Gorczyca and Rosół (2011) relationships between the control current $i(t)$ in coils and the static frictional damping torque $M_D^F(i(t))$ and the viscous damping coefficient $d(i(t))$ are respectively presented in Figs. 4a and 4b. For the maximum braking torque equal to 4 Nm obtained for the control current 1 A, declared by the producer of the considered rotary brake, by means of the identification results plotted in these figures and for the selected constant control current values, using formula (2.1), one can determine damping torque characteristics of the magneto-rheological rotary brake or damper. Such exemplary characteristics are shown in Fig. 5.
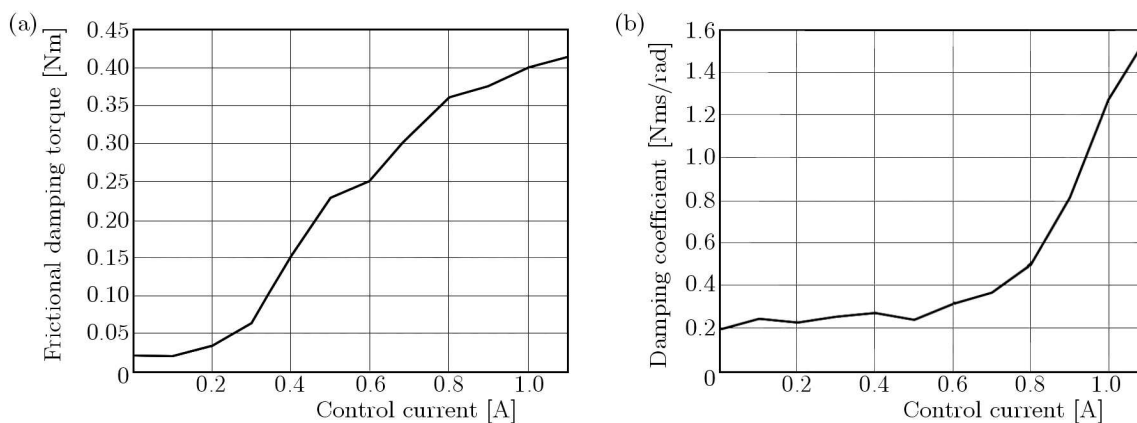

Fig. 4. Experimentally identified by Gorczyca and Rosół (2011) relationships between the control current and the static frictional damping torque (a) and the viscous damping coefficient (b) of the MRF

From the respective plots in Figs. 4 and 5, it follows that the contribution of the static frictional damping torque component progressively increases with the rise of the control current. This property of the rotary magneto-rheological dampers can be essential for semi-active control of torsional vibrations.
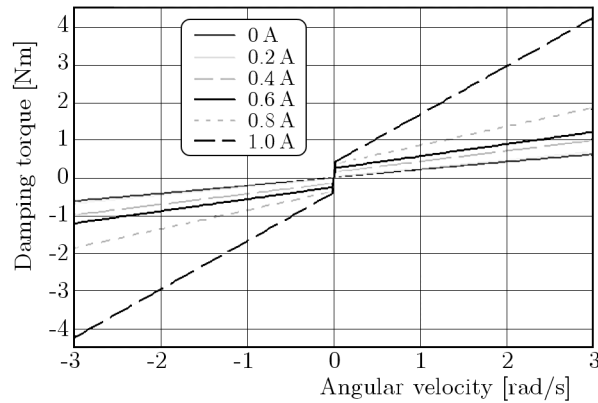
Fig. 5. Damping torque characteristics of the rotary magneto-rheological device
for constant control currents

3. Assumptions for the mechanical models and formulation of the problem

In order to increase reliability of the obtained theoretical results, the investigations are performed by means of the hybrid and the classical finite element (FEM) structural electro-mechanical models of the considered real laboratory drive system presented in Fig. 1. These two models consisting of rigid bodies and continuous or discretized deformable finite elements, respectively, are employed here for eigenvalue analyses as well as for numerical simulations of torsional vibrations of the drive system coupled with electrical vibrations in the motor windings. The common structure of the assumed hybrid and finite element mechanical model is shown in Fig. 6.
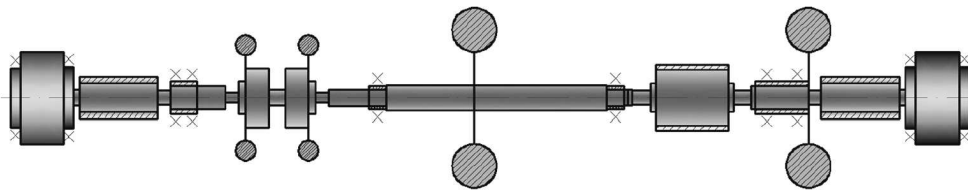

Fig. 6. The structure of hybrid and finite element mechanical model of the drive system

In the hybrid model, successive cylindrical segments of the stepped rotor-shaft are substituted by the cylindrical macro-elements of continuously distributed inertial-visco-elastic properties, as presented in Fig. 6. However, in the finite element model, these continuous macro-elements have been discretized with a proper mesh density assuring a sufficient accuracy of the results. Since in the real drive system the electric motor coils and coupling disks are attached along some rotor-shaft segments by means of shrink-fit connections, the entire inertia of such components is increased, whereas usually the shaft cross-sections are only affected by elastic deformations due to transmitted loadings. Thus, the corresponding visco-elastic macro-elements in the hybrid model and the discretized finite elements in the FEM model must be characterized by geometric cross-sectional polar moments of inertia J_{Ei} responsible for their elastic and inertial properties as well as by separate layers of the polar moments of inertia J_{Ii} responsible for their inertial properties only, $i = 1, 2, \ldots, n$, where n is the total number of macro-elements in the considered hybrid model, Fig. 6. Moreover, on the actual operational temperature T_i can depend values of Kirchhhoff's moduli G_i of the rotor-shaft material of the density ρ for each i-th macro-element representing the given rotor-shaft segment. In the proposed hybrid and FEM model of the laboratory drive system, the inertias of the inertial disks are represented by rigid bodies attached to the appropriate macro-element extreme cross-sections, which should assure a reasonable accuracy for practical purposes.

Torsional motion of cross-sections of each visco-elastic macro-element in the hybrid model is governed by hyperbolic partial differential equations of the wave type

$$G_i(T_i)J_{Ei}\Big(1 + \tau\frac{\partial}{\partial t}\Big)\frac{\partial^2\theta_i(x,t)}{\partial x^2} - c_i\frac{\partial\theta_i(x,t)}{\partial t} - \rho(J_{Ei} + J_{Ii})\frac{\partial^2\theta_i(x,t)}{\partial t^2} = q_i\big(x,t,\theta_i(x,t)\big) \quad (3.1)$$

where $\theta_i(x,t)$ is the angular displacement with respect to the shaft rotation with the average angular velocity Ω, τ denotes the retardation time in the Voigt model of material damping and c_i is the coefficient of external (absolute) damping. The response-dependent external active and passive torques are continuously distributed along the respective macro-elements. These torques are described by the two-argument function $q_i(x,t,\theta_i(x,t))$, where x is the spatial co-ordinate and t denotes time. Mutual connections of the successive macro-elements creating the stepped shaft as well as their interactions with the rigid bodies are described by equations of boundary conditions. These equations contain geometrical conditions of conformity for rotational displacements of the extreme cross sections of the adjacent neighbouring elastic macro-elements. The second group of boundary conditions are dynamic ones which contain equations of equilibrium for external and control torques as well as for inertial, elastic and external damping moments. For example, action of the magneto-rheological dampers is also described by the following dynamic boundary conditions

$$\begin{aligned}
-&G_j(T_j)J_{Ej}\Big(1 + \tau\frac{\partial}{\partial t}\Big)\frac{\partial\theta_j(x,t)}{\partial x} + G_{j-1}(T_{j-1})J_{E,j-1}\Big(1 + \tau\frac{\partial}{\partial t}\Big)\frac{\partial\theta_{j-1}(x,t)}{\partial x} \\
&+ d_j\big(i(t)\big)\Delta\Omega_j(t) = -M_D^F\big(i(t)\big) \\
&J_j\frac{d\Omega_j(t)}{dt} - d_j\big(i(t)\big)\Delta\Omega_j(t) = M_D^F\big(i(t)\big)
\end{aligned} \qquad (3.2)$$

where

$$\Delta\Omega_j(t) = \Omega(t) + \frac{\partial\theta_j(x,t)}{\partial t} - \Omega_j(t) \qquad \text{for} \qquad x = \sum_{k=1}^{j-1} l_k$$

$\Omega_j(t)$ denotes the rotational speed of the magneto-rheological damper inertial ring of the polar mass moment of inertia J_j, l_k are the lengths of successive macro-elements in the hybrid model, and the macro-element number j determines the position of the damper in the drive system model.

The solution for forced vibration analysis has been obtained using the analytical--computational approach described e.g. in Szolc (2000). Solving the differential eigenvalue problem and applying the Fourier solution in form of series in the orthogonal eigenfunctions leads to a set of uncoupled modal equations for time coordinates $\xi_m(t)$

$$\ddot{\xi}_m(t) + (\beta + \tau\omega_m^2)\dot{\xi}_m(t) + \omega_m^2\xi_m(t) = \frac{1}{\gamma_m^2}Q_m(t) \qquad m = 1, 2, \ldots \qquad (3.3)$$

where ω_m are the successive natural frequencies of the drive system, β denotes the coefficient of external damping assumed here as a proportional damping to the modal masses γ_m^2 and $Q_m(t)$ are the modal external excitations.

The damping torques $M_D\big(i(t)\big)$ expressed by (2.1) can be regarded as the response-dependent control external excitations. Then, similarly as e.g. in Szolc (2000), upon transformation of them into the space of modal coordinates $\xi_m(t)$ and substitution into independent equations (3.3), the following set of coupled modal equations is yielded

$$\mathbf{M}_0\ddot{\mathbf{r}}(t) + \mathbf{D}\Big(d_j\big(i(t)\big), \dot{\mathbf{r}}(t)\Big)\dot{\mathbf{r}}(t) + \mathbf{K}_0\mathbf{r}(t) = \mathbf{F}(t, \dot{\mathbf{r}}(t)) \qquad (3.4)$$

where

$$\mathbf{D}(\dot{\mathbf{r}}(t)) = \mathbf{D}_0 + \mathbf{D}_C\Big(d_j(i(t)), \dot{\mathbf{r}}(t)\Big)$$

The symbols $\mathbf{M}_0$, $\mathbf{K}_0$ and $\mathbf{D}_0$ denote, respectively, the constant diagonal modal mass, stiffness and damping matrices. The full matrix $\mathbf{D}_C\Big(d_j(i(t)), \dot{\mathbf{r}}(t)\Big)$ plays here a role of the semi-active control matrix and the symbol $\mathbf{F}(t, \dot{\mathbf{r}}(t))$ denotes the response-dependent external excitation vector due to the electro-magnetic torque generated by the electric motor and due to the retarding torque produced by the electric brake. The Lagrange coordinate vector $\mathbf{r}(t)$ consists of the unknown time functions $\xi_m(t)$ in the Fourier solutions, $m = 1, 2, \ldots$. The number of equations (3.4) corresponds to the number of torsional eigenmodes taken into consideration in the range of frequency of interest. These equations are mutually coupled by the out-of-diagonal terms in the matrix $\mathbf{D}$ regarded as external excitations expanded in series in the base of orthogonal analytical eigenfunctions. A fast convergence of the applied Fourier solution enables us to reduce the appropriate number of the modal equations to be solved in order to obtain a sufficient accuracy of results in the given range of frequency. Here, it is necessary to solve only 6-10 coupled modal equations (3.4), contrary to the classical one-dimensional rod finite element formulation leading in general to a relatively large number of equations of motion in the generalized coordinates.

For the assumed analogous finite element model, the mathematical description of its motion has the classical form of a set of coupled ordinary differential equations

$$\mathbf{M}\ddot{\mathbf{s}}(t) + \mathbf{C}\Big(d_j(i(t)), \dot{\mathbf{s}}(t)\Big)\dot{\mathbf{s}}(t) + \mathbf{K}\mathbf{s}(t) = \mathbf{F}(t, \dot{s}(t)) \tag{3.5}$$

where $\mathbf{s}(t)$ denotes the vector of generalized co-ordinates $s_j(t)$, $\mathbf{M}$, $\mathbf{C}\Big(d_j(i(t)), \dot{\mathbf{s}}(t)\Big)$ and $\mathbf{K}$ are respectively the mass, damping and stiffness matrices and $\mathbf{F}$ denotes the time- and system response-dependent external excitation vector. By means of equations (3.5), numerical simulations of the forced torsional vibrations for the passive and controlled system can be carried out. In order to determine natural frequencies and eigenvectors for the FEM model of this drive system, it is necessary to reduce (3.5) into the so called standard eigenvalue problem.

4. Modelling of the electrical external excitation generated by the servo-asynchronous motor

The torsional vibrations of the drive system usually result in significant fluctuation of rotational speed of the rotor of the driving electric motor. Such oscillation of the angular velocity superimposed to the average rotor rotational speed causes more or less severe perturbation of the electro-magnetic flux and thus additional oscillation of the electric currents in the motor windings. Then, the generated electro-magnetic torque is also characterized by an additional variable in time components which induce torsional vibrations of the drive system. According to the above, the mechanical vibrations of the drive system become coupled with the electrical vibrations of the currents in the motor windings. Such coupling is often complicated in character and thus computationally troublesome. Because of this reason, till present, majority of authors simplify the matter regarding the mechanical vibrations of drive systems and the electric current vibrations in motor windings as mutually uncoupled. Then, mechanical engineers apply the electro-magnetic torques generated by the electric motors as *a priori* assumed excitation functions of time or the rotor-to-stator slip, see e.g. Laschet (1988), usually determined by means of experimental measurements for a variety of dynamical behaviour of the given electric motor. However, electricians thoroughly model the generated electro-magnetic torques basing on electric current flows in the electric motor windings, but they usually reduce the mechanical drive

system to one or seldom to a few rotating rigid bodies. In many cases, such simplifications yield insufficiently exact results, both for the mechanical and the electrical part of the investigated object.

In order to develop a proper control algorithm for the given vibrating drive system, the electro-magnetic external excitation produced by the motor should be described possibly accurately, and thus the electro-mechanical coupling between the electric motor and the torsional train ought to be taken into consideration. According to the above, apart from the sufficiently realistic mechanical models of the vibrating object, it is also necessary to introduce a proper mathematical model of the electric motor. In the considered case of the symmetrical three-phase asynchronous motor, electric current oscillations in its windings are described by six voltage equations transformed next into the system of four Park's equations in the so called $\alpha\beta - dq$ reference system, which can be found e.g. in Shi *et al.* (1999). Then, the electro-magnetic torque generated by such a motor can be expressed by the following formula

$$T_{el} = \frac{3}{2}pM(i_\beta^s i_d^r - i_\alpha^s i_q^r) \tag{4.1}$$

where M denotes the relative rotor-to-stator coil inductance, p is the number of pairs of the motor magnetic poles and i_α^s, i_β^s are the electric currents in the stator reduced to the electric field equivalent axes α and β and i_d^r, i_q^r are the electric currents in the rotor reduced to the electric field equivalent axes d and q, Shi *et al.* (1999). From the abovementioned system of voltage equations as well as from formula (4.1), it follows that the coupling between the electric and the mechanical system is non-linear in character, which leads to a very complicated analytical description resulting in rather harmful computer implementation. Thus, this electro-mechanical coupling has been realized here by means of the step-by-step numerical extrapolation technique, which for relatively small direct integration steps for equations (3.4) and (3.5) results in very effective, stable and reliable results of computer simulation.

5. Computational and experimental example

As described above, the structure and measurement equipment of the experimental test-rig as well as its mathematical models enable application of various semi-active control algorithms for attenuation of torsional vibrations. From the theoretical investigations carried out in Szolc *et al.* (2010), for the considered concept of torsional vibration control using the rotary magneto-rheological dampers, it follows that for the drive system affected by dynamic loading characterized by clear, predominant frequency components the open-loop semi-active control is similarly effective in suppression of vibration amplitudes as the closed-loop one. It is to emphasize that generally the open-loop control strategy is much simpler and cheaper in practical applications in industrial conditions. Thus, the open-loop semi-active control strategy is going to be used here as an introductory approach. In this case, the problem reduces to a selection of the *a priori* assumed optimal damping parameters $M_D^F(i(t))$ and $d(i(t))$ in (2.1) realized by the rotary magneto-rheological dampers. In order to assume an optimum constant value of the viscous damping coefficient $d(i(t))$ and, in this way, an optimum value of the control current applied to the rotary dampers according to the characteristic shown in Fig. 4b, the following criterion has to be satisfied

$$d_0 = \arg\min_d \max_f FRF_r(f, d) \tag{5.1}$$

Here, the value of d_0 is optimal with respect to the frequency response function (FRF) of the damped drive system excited with the predominant excitation frequency f of the transmitted loading. From expression (5.1) it follows that the selection of an optimal value of the damping

coefficient is based on the dynamic characteristic of the considered drive system in form of the frequency response function. But in general, it is to emphasize that the frequency response functions can be determined for linear systems with constant damping coefficients, which in the considered case requires neglecting the frictional components $M_D^F(i(t))$ of the damping characteristics depicted in Fig. 5. Taking into account the relatively small contribution of this kind of damping in comparison with the viscous one, such simplification can be accepted, in particular when the criterion for control strategy elaboration is sought. The frequency response function determined for the investigated laboratory drive system excited by the electro-magnetic brake and for the omitted $M_D^F(i(t))$ in (2.1) is shown in Fig. 7. Here, in order to obtain a satisfactory agreement between the measured and calculated first natural frequency values, the mechanical model of the drive system must have been properly tuned-up. According to Laschet (1988), this target was achieved by means of appropriate parameter modification of the hybrid model macro-elements characterized by the greatest potential eigenenergy corresponding to the system successive natural frequencies. From the presented plot, it follows that for the system dynamical parameters, the frequency response function rapidly falls with the rise of the damping coefficient to rich its minimum for ca. 1.0-1.5 Nms/rad per one rotary damper at the excitation frequency 54.4 Hz corresponding to the first torsional eigenvibration mode. Then, further increase of the damping coefficient leads to a slow rise of the response amplitude, which can be substantiated by a gradual locking-up of the rotary dampers manifesting themselves in sticking of the damper inertial rings to the torsionally vibrating shaft. Then, the damping effect vanishes and the thus increased the entire mass moment of inertia results in a remarkably slight decrease of the first natural frequency below 50 Hz, see Fig. 7. As it follows from the identified by Gorczyca and Rosół (2011) characteristics of the rotary magneto-rheological damper depicted in Figs. 4a and 4b, the optimal value of the damping coefficient $d_0(i_0) \approx 1.0 - 1.5$ Nms/rad can be realized by the control current $i_0 \approx 1.0$ A.
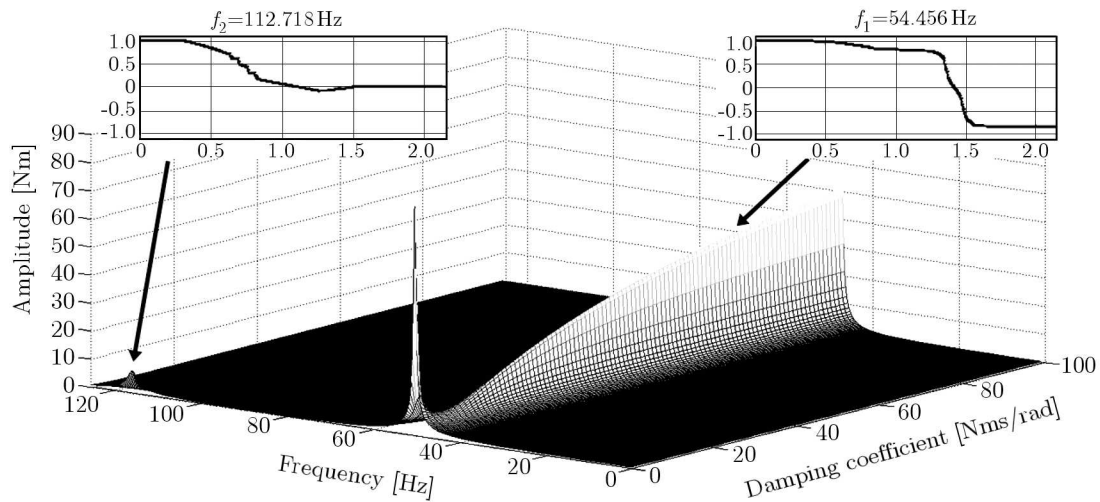

Fig. 7. The frequency response function of the laboratory drive system model

The determined in this way approach to the open-loop semi-active control of torsional vibrations using the magneto-rheological rotary dampers is going to be experimentally and theoretically verified. Here, steady-state operating conditions of the drive system are investigated for its constant average rotational speed, where an external harmonic excitation in the frequency range 0-150 Hz with an amplitude equal to 0.25 of the nominal transmitted torque is generated by the electric brake. It is worth noting that this excitation frequency range contains the first two torsional eigenmodes, as one can notice from the appropriate plots in Fig. 7. Moreover, it is to remember as well that in such operating conditions, the driving asynchronous motor generates also an approximately harmonic electro-magnetic torque component of the same frequency

as that induced by the power receiver, which is a consequence of the rotor-to-stator electro-
-magnetic flux interaction described e.g. by the circuit model in the form of Park's equations,
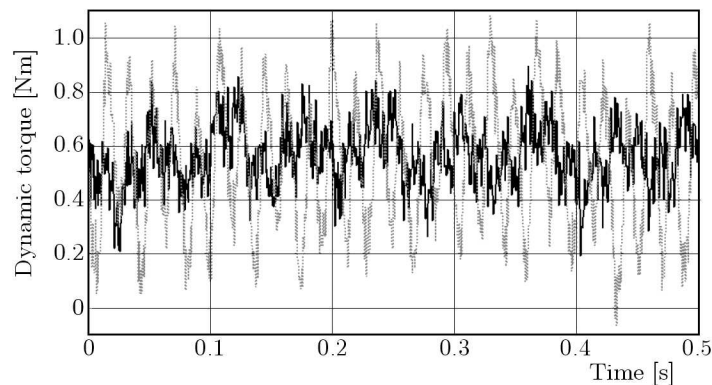see Shi *et al.* (1999) and Szolc and Pochanke (2012) and other numerous publications.

Fig. 8. Measured time histories of the dynamic torque for the passive (grey)
and controlled system (black)

In Fig. 8, time histories of the measured dynamic torques registered by the torque-meter I
between the driving motor and the magneto-rheological dampers, see Fig. 1, obtained respecti-
vely for the passive system (grey line) and for the optimally controlled system (black line) with
the control current $0.5\,\text{A}$, both under resonant excitation with the abovementioned frequen-
cy $\sim 54\,\text{Hz}$ are presented. Analogous results determined by means of numerical simulations are
shown in Fig. 9, where basing on the magneto-rheological damper characteristics presented in
Figs. 4 and 5, in the case of the passive system, i.e. for the zero control current (grey dashed line)
$M_D^F(i_0) = 0.02\,\text{Nm}$, $d_0(i_0) = 0.2\,\text{Nms/rad}$ in (2.1), (3.2), (3.4) and (3.5) was assumed and for
the two semi-actively controlled cases, respectively: $M_D^F(i_0) = 0.23\,\text{Nm}$, $d_0(i_0) = 0.25\,\text{Nms/rad}$
for the control current $0.5\,\text{A}$ (grey solid line) and $M_D^F(i_0) = 0.4\,\text{Nm}$, $d_0(i_0) = 1.3\,\text{Nms/rad}$ for
the optimal control current $1\,\text{A}$ (black line). Both from the experimentally and theoretically
obtained plots, it follows that for the most inconvenient resonant operating conditions the rota-
ry magneto-rheological dampers suppress torsional vibration amplitudes in the considered shaft
segment more than twice. This result has been confirmed by the experimentally and theoretically
obtained amplitude characteristics using FFT in the abovementioned excitation frequency range
0-150 Hz. The respective plots determined by means of measurements are shown in Fig. 10a, and
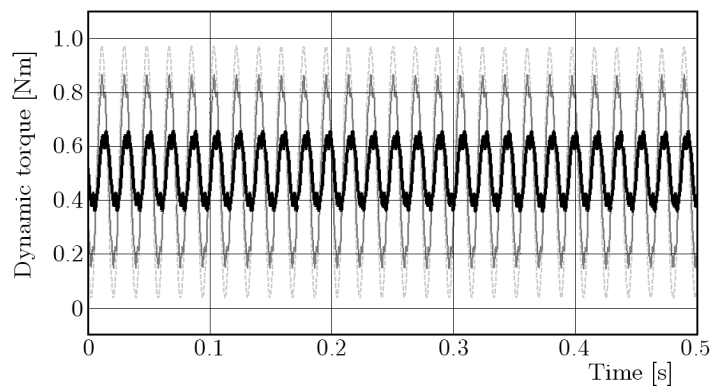these obtained by the use of computations are presented in Fig. 10b.

Fig. 9. Calculated time histories of the dynamic torque for the passive (dashed grey)
and controlled system (solid grey – $0.5\,\text{A}$, black – $1.0\,\text{A}$)
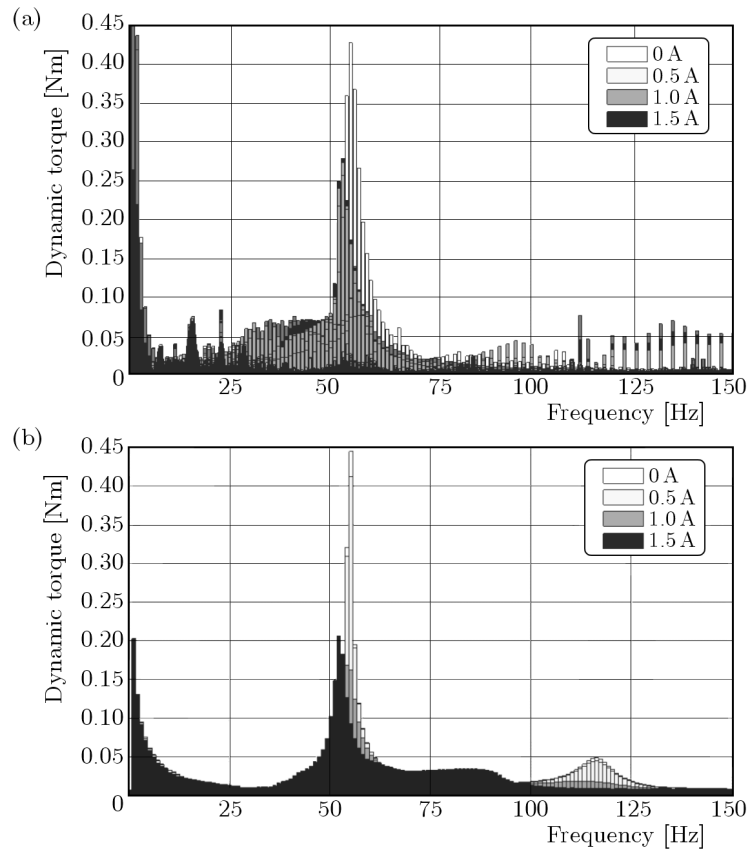
Fig. 10. Amplitude characteristics of the dynamic torque transmitted by torque-meter I shaft segment for the passive and the semi-actively controlled system obtained using experiment (a) and simulation (b)

From the obtained and illustrated in this way experimental and theoretical findings, it follows that beyond some interferences generated by the electric brake at the excitation frequencies ~ 16 and ~ 22 Hz, see Fig. 10a, a very good qualitative agreement between the measured and calculated results has been achieved, taking into account the similarity of the respective extreme values and corresponding to them interaction frequencies. However, the most significant torsional vibration attenuation effects have been obtained for the control current 0.5 A during measurements and for 1 A by the use of computations. It means that the real minimum vibration amplitudes occurred for different damping parameters $d_0(i_0)$ and $M_D^F(i_0)$ according to the characteristics of the MRF in LORD RD-2087-01 device determined by Gorczyca and Rosół (2011). Nevertheless, in both cases, for greater control current values, i.e. 1.5 A, and for the corresponding greater damping parameter values, remarkably greater torsional vibration amplitudes are observed, the respective maxima of which correspond to smaller interaction frequencies, see Fig. 10. Here, the control current 1.5 A is the maximum admissible current value, for which the corresponding damping parameters $d_0(i_0)$ and $M_D^F(i_0)$ must have been heuristically extrapolated using the characteristics in Fig. 4. Then, due to a rise in the drive system entire mass moment of inertia caused by almost hard 'sticking' of the damper inertial rings to the torsionally vibrating shaft, the rotary dampers start to be gradually locked-up. It results in a weaker dissipation effectiveness and in a decreasing of the drive system fundamental natural frequencies from 54.4 Hz to ~ 49 Hz in the case of the first eigenmode and from 112.7 Hz to ~ 85 Hz in the case of the second eigenmode, as shown in Figs. 10a and 10b. According to the above, one can state that the identification result achieved by Gorczyca and Rosół (2011) could be applied here as an introductory approximation indicating only a realistic range of damping parameter values for numerical simulations. The obtained discrepancies

between the real and theoretical damping parameters of the MRF can be caused by the different operation mode of the LORD RD-2087-01 device – as a brake in Gorczyca and Rosół (2011) and as a rotary damper in the presented paper. It is to notice that analogous damping parameter identification of the LORD RD-2087-01 device operating here as the rotary damper would lead to essential difficulties in measuring rotational velocities of the damper inertial rings. Moreover, it is worth noting that both the measurements and computations have indicated remarkably grater vibration amplitudes in the vicinity of the fundamental resonance, i.e. 54.4 Hz, registered for the controlled cases in comparison with the passive one. As it follows from the results of numerous auxiliary numerical simulations, these effects can be explained by a rather negative influence of the frictional components of MRF damping properties, when the mechanical system is operating close to the resonance and beating effects usually occur. Moreover, all experimentally and theoretically obtained amplitude characteristics shown in Figs. 10a and 10b indicate relatively high torsional oscillations in the range of small excitation frequencies, i.e. within 0-3 Hz. As it follows from proper investigations carried out by Szolc and Pochanke (2012), these high vibration amplitudes result from the low-frequency electro-mechanical interaction between the driving asynchronous motor torque and the driven mechanical system.

Finally, it is to emphasize that the carried out investigation of the suppression ability of the drive system torsional vibrations using the rotary magneto-rheological dampers was actually based on comparisons of the uncontrolled and controlled dynamic responses observed in the shaft segment corresponding to location of torque-meter I, see Fig. 1. But from the shapes of the first two system eigenfunctions shown in Fig. 7, it follows that because of the much greater modal displacement gradients the largest dynamic torque amplitudes are expected in the middle of the considered drive train length, where any torque-meter is installed. Thus, the abovementioned differences of torsional vibration amplitudes observed in the cases of the controlled system and of the passive one can serve us as an experimentally verified measure of the amplitude suppression ability of the rotary magneto-rheological dampers. However, the greatest differences between the dynamic response amplitudes of the passive and semi-actively controlled system occurred in the middle part of the drive train, i.e. in the vicinity of the overload coupling, see Fig. 1. In Fig. 11, in an identical way as in Fig. 10b, the calculated amplitude characteristics of the dynamic torque transmitted by the most heavily affected shaft segment located in this part of the considered system are demonstrated. But here, in the resonant operating conditions, the semi-active control performed using the theoretical optimum control current 1 A results in four times smaller torsional vibration amplitudes than in the case of the passive system. A reliability of this issue can be regarded as semi-directly experimentally verified by means of the results discussed above and shown in Figs. 8-10, obtained for the shaft segment corresponding to the location of torque-meter I.
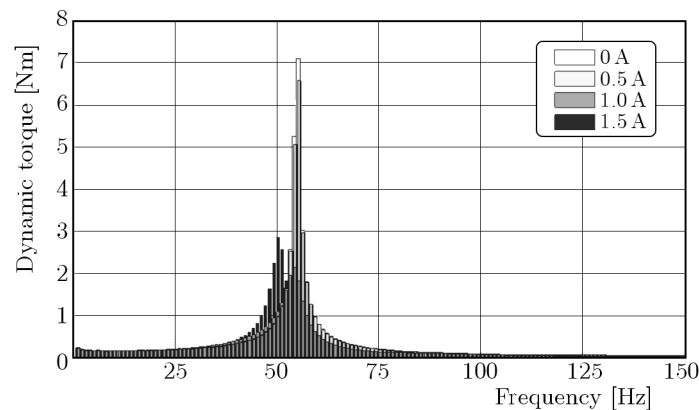

Fig. 11. Amplitude characteristics of the dynamic torque transmitted by the most heavily affected shaft segment for the passive and semi-actively controlled system obtained using simulation

6.   Conclusions

In the paper, semi-active control of steady-state torsional vibrations of a laboratory drive system driven by an asynchronous motor has been computationally and experimentally performed by means of rotary dampers with an MRF. From the performed and described above experimental and theoretical investigations, it follows that the rotary magneto-rheological dampers can effectively suppress torsional vibrations of drive systems of several machines and mechanisms. The optimum control realized by means of the *a priori* assumed control current, and in this way damping parameters, can essentially reduce steady-state torsional vibrations of the successive shaft segments. From the results of measurements and computations it follows that for properly selected control currents based on the respective minimum of the frequency response function determined for the considered mechanical system, the rotary actuators with the MRF can minimize the torsional vibration level many times, particularly for the resonance operating conditions, e.g. corresponding to the first fundamental eigenmode. It is to emphasize that the presented open-loop approach demonstrating all advantages of the semi-active control strategy is relatively easy to be implemented into real technical objects. The results of measurements have been quite successfully confirmed and explained by the analogous results of numerical simulations obtained by means of both applied electro-mechanical models of the considered object. This fact substantiates the reliability and satisfactory accuracy of the proposed control technique for practical engineering applications. In the next steps of research in this field, the closed-loop semi-active control is going to be realized and tested for various values of the mass-moment of inertia of the magneto-rheological damper inertial rings installed to the drive system under transient and steady-state operating conditions excited by several external loadings.

References

1. GORCZYCA P., ROSÓŁ M., 2011, A semi-active suspension system model, *Proceedings of the 10th Conference on Active Noise and Vibration Control Methods*, Cracov 2011, 206-213

2. LASCHET A., 1988, *Simulation von Antriebssystemen*, Berlin, London, N-Y: Springer-Verlag

3. MAKOWSKI M., KNAP L., GRZESIKIEWICZ W., 2011, Modeling and parameters identification of controlled magneto-rheological dampers (in Polish), *Modelowanie Inżynierskie*, **41**, 261-269

4. MIKUŁOWSKI G., HOLNICKI-SZULC J., 2007, Adaptive landing gear concept – feedback control validation, *Smart Materials and Structures*, **16**, 6, 2146-2158

5. PRĘGOWSKA A., KONOWROCKI R., SZOLC T., 2012, Experimental verification of the semi-active control concepts for torsional vibrations of the electro-mechanical system using rotary magneto-rheological actuators, *Vibrations in Physical Systems*, **25**, 329-334

6. PRZYBYŁOWICZ P.M., 1995, Torsional vibration control by active piezoelectric system, *Journal of Theoretical and Applied Mechanics*, **33**, 4, 809-823

7. SPENCER JR. B.F., DYKE S.J., SAIN M.K., CARLSON J.D., 1997, Phenomenological model for magnetorheological dampers, *Journal of Engineering Mechanics, ASCE*, **123**, 3, 230-238

8. SHI K.L., CHAN T.F., WONG Y.K., HO L.S., 1999, Modelling and simulation of the three-phase induction motor using SIMULINK, *International Journal of Electrical Engineering Education*, **36**, 163-172

9. SZOLC T., 2000, On the discrete-continuous modeling of rotor systems for the analysis of coupled lateral-torsional vibrations, *International Journal of Rotating Machinery*, **6**, 2, 135-149

10. SZOLC T., JANKOWSKI Ł., POCHANKE A., MAGDZIAK A., 2010, An application of the magneto-rheological actuators to torsional vibration control of the rotating electro-mechanical systems, *Proceedings of the 8th IFToMM International Conference of Rotor Dynamics, KIST*, 488-495

11. Szolc T., Jankowski Ł., Pochanke A., Michajłow M., 2011, Vibration control of the coal pulvelizer geared drive system using linear actuators with the magneto-rheological fluid, *Proceedings of the 9th International Conference on Vibrations in Rotating Machines SIRM 2011*, Darmstadt, Germany, Paper ID-46

12. Szolc T., Michajłow M., Konowrocki R., 2013, On electromechanical dynamic coupling effects in the semi-actively controlled rotating machine drive system driven by the induction motor, *Proceedings of the 10th Int. Conference on Vibrations in Rotating Machines SIRM 2013*, Berlin, Germany, Paper ID-258

13. Szolc T., Pochanke A., 2012, Analytical-computational approach to dynamic investigation of the electro-mechanical coupling effects in the rotating systems driven by asynchronous motors, *Proceedings of the 10th IMechE International Conference on Vibrations in Rotating Machinery*, One Birdcage Walk, London, UK, IMechE Paper C1326/066,753-764

14. Wang J., Meng G., 2005, Study of the vibration control of a rotor system using a magnetorheological fluid damper, *Journal of Vibration and Control*, **11**, 263-276